Accepted Manuscript

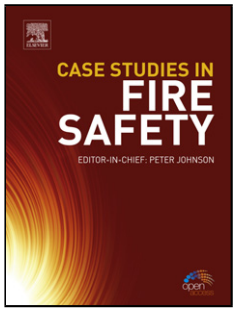

Title: Formation of an incombustible oxide film on a molten Mg-Al-Ca alloy

Authors: Shin-ichi Inoue, Michiaki Yamasaki, Yoshihito Kawamura

PII: S0010-938X(16)30554-6
DOI: http://dx.doi.org/doi:10.1016/j.corsci.2017.01.026
Reference: CS 6991

To appear in:

Received date: 13-8-2016
Revised date: 24-1-2017
Accepted date: 26-1-2017

Please cite this article as: {http://dx.doi.org/

Formation of an incombustible oxide film on a molten Mg-Al-Ca alloy

Shin-ichi Inoue[a, *], Michiaki Yamasaki[a, b], and Yoshihito Kawamura[a]

[a]Magnesium Research Center, Kumamoto University, 2-39-1 Kurokami, Chuo-ku, Kumamoto, 860-8555, Japan

[b]School of Mechanical and Mining Engineering, The University of Queensland, St Lucia, Brisbane, Qld 4072, Australia

* Corresponding author. e-mail: shinoue7@kumamoto-u.ac.jp, fax: +81-96-342-3721

Graphical abstract

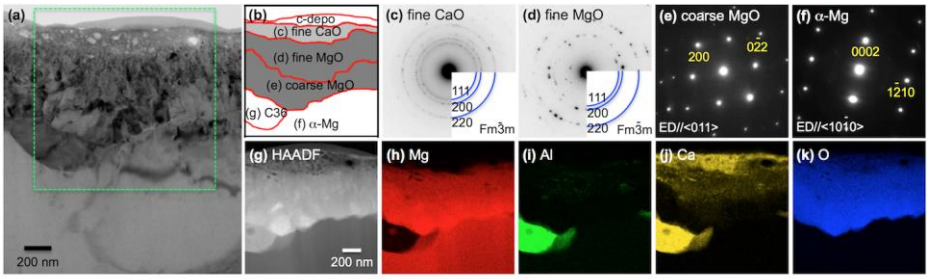

(a) TEM image of a FIB-prepared cross-section of the film formed on the alloy after solidification of $Mg_{85}Al_{10}Ca_5$ melt. (b) Schematic diagram of layered structure of the oxide film. SAED patterns obtained from each region; (c) outer layer, (d) intermediate layer, (e) innermost layer, and (f) underlying alloy. (g) HAADF image and EDS element maps for (h) Mg, (i) Ca, (j) Al, (k) O.

Highlights

- The nonflammable $Mg_{85}Al_{10}Ca_5$ alloy exhibits a high ignition temperature of 1436 K.
- The oxide film formed on the molten alloy was found to be a three-layered structure.
- The outer layer of the three-layered structure consists of fine CaO grains.
- The incombustibility may be due to the formation of the fine CaO outer layer.

Abstract

A nonflammable Mg-10Al-5Ca (at.%) alloy that can be melted in air without a cover gas or flux is developed. The alloy immediately forms a protective oxide film consisting of three layers, a fine CaO outer layer, a fine MgO intermediate layer, and a coarse MgO innermost layer. The anionic volume ratio of the CaO/MgO interface is 1.48. This interface ratio is sufficiently large to suggest the generation of a strong compressive force in the CaO layer. The dense, uniform fine CaO layer may act as a protective layer preventing the diffusion of oxygen.

keywords: A. magnesium, A. calcium, B. TEM, C. oxidation, C. high-temperature corrosion

1. Introduction

Among the lightweight structural metallic materials, Mg alloys have been attracting keen attention as key engineering materials for automobile, railway, and aerospace applications, where weight reduction is of particular concern [1]. On the other hand, however, it is widely perceived that, having low oxidation resistance, Mg alloys are liable to burn easily. In fact, easy ignition may be a critical problem in all conceivable Mg alloy applications. Nevertheless, the Federal Aviation Administration (FAA) in the USA, aerospace specification committees, and national institutes are conducting a review of the existing ban on the use of Mg alloys in aircraft cabins in recognition of the light weight of Mg alloys [2-4]. In addition, several studies have been undertaken by an aircraft company, along with its collaborators, to define an appropriate methodology for the development of nonflammable Mg alloys [5, 6].

Meanwhile, we have witnessed the development of several nonflammable Mg alloys through the addition of reactive metal elements [7]. It has long been known that Be imparts appreciably greater oxidation resistance to Mg alloys when added in minute amounts [8-13]. Ca or CaO similarly inhibits the ignition and burning of molten Mg alloys [13-21]. Rare earth (RE)-containing Mg alloys have also been attracting wide attention [5-7, 20-24]. Zeng et al. reported that Be promotes the formation of an inner layer comprising a mixture of MgO and BeO in the surface oxide film, thereby enabling the alloys to exhibit excellent ignition-proof performance [11]. You and coworkers reported that adding Ca to Mg alloys resulted in the formation of a two-layered oxide film with the outer layer mainly consisting of CaO and the inner layer comprising a mixture of CaO and MgO during high-temperature oxidation [13, 16, 17]. RE elements form an RE oxide film on alloys with moderate anti-combustibility [5-7, 20-24]. Among these alloys, Ca-containing Mg alloys are the most promising for use as nonflammable lightweight Mg alloys in aerospace applications [1]. Unfortunately, however, Mg alloys with a Ca content of more than 1 at.% Ca are embrittled by intermetallic compounds formed during alloying, preventing their use [25]. Therefore, the development of the Ca-containing Mg alloy system has been constrained within a narrow range of Ca concentrations [25-30]. To overcome this problem, researchers have drawn on rapidly solidified powder metallurgy (RS P/M) processing, succeeding in the fabrication of Mg-20Al-10Ca (at.%) RS P/M alloy with high mechanical performance in 2000 [31]. The new alloy was found to have several desirable qualities, including a tensile strength of 600 MPa with reasonable elongation. Recently, a high-strength, nonflammable Mg-10Al-5Ca (at.%) alloy has been developed using conventional casting and extrusion techniques [32]. This alloy is composed of fine grains with α-Mg, C36, and C14 phases, and has high strength and ductility. In addition, it had a high ignition temperature of more than 1360 K [32].

Fortunately, as mentioned above, there have been several excellent studies concerning the controlling of the ignition temperature of Ca-containing Mg alloys [13-21]. Choi et al. reported that the ignition temperatures of AZ91 alloys containing 0.3-5.0 wt.% Ca increase with increasing Ca content [13]. However, the ignition temperatures of Mg alloys that containing more than 5 wt.% Ca have not yet been determined. Therefore, it is important to measure the ignition temperature of the high-Ca-concentration Mg-10Al-5Ca (Mg-10.64Al-7.9Ca (wt.%)) alloy and to clarify the mechanism of its incombustibility. With this background, this study was carried out to elucidate the role of Ca in modifying the structure and composition of the oxide film formed on molten Mg-10Al-5Ca alloy. A focused ion beam (FIB)-prepared cross section of a specimen obtained from the film formed on the alloy was observed by transmission electron spectroscopy (TEM) after the solidification of molten Mg-10Al-5Ca alloy.

2. Material and methods

Mg-10Al-5Ca alloy specimens were prepared by the high-frequency induction melting of pure Mg (99.99 wt.%), Al (99.99 wt.%), and Ca (99.9 wt.%) in a carbon crucible. The molten alloys were maintained at 1023 K and cast in an argon atmosphere.

The ignition temperature measurements were performed using thermogravimetry/differential thermal analysis apparatus (TG-DTA, SII TG/DTA-6300). The cast ingot was cut into disc-shaped specimens of 3.8 mm diameter and 0.4 mm thickness. The surface of the specimens was mechanically ground with #4000 SiC paper. A disc-shaped specimen was placed in an alumina pan, and then heated with a heating rate of 50 K/min in air with 20% humidity at atmospheric pressure. The specimen temperature was measured by a thermocouple installed underneath the alumina pan.

The microstructure of the cast Mg-10Al-5Ca alloy was observed using a scanning electron microscope (SEM, JEOL JIB-4601F). The SEM specimens were polished by paper lapping and ion milling (JEOL SM-09010). The microstructures were characterized by electron backscatter diffraction (EBSD) using orientation imaging microscopy software (TSL Solutions K.K., OIM ver. 6). Chemical compositions were analyzed using an energy-dispersive X-ray spectroscopy (EDS) system installed in the SEM.

The structure of the oxide film was investigated by grazing incidence X-ray diffractometry (GI-XRD, Bruker D8 Discover) and transmission electron microscopy (TEM, JEOL JEM-2100F). Prior to the GI-XRD measurement and TEM observations, the plate-shaped Mg-10Al-5Ca alloy specimens (7 x 5 x 1 mm) were remelted at 973 K for 10 min in a muffle furnace and then solidified in air. GI-XRD data were collected in the 2θ diffraction angle

range of 20-90° using Cu*K*α radiation at an incident angle of 0.2°. The step width and counting time in each step were 0.02° and 10 s, respectively. TEM and scanning TEM (STEM) observations were conducted on a cross section of the oxide film formed on the molten Mg-10Al-5Ca alloy. An FIB system (FEI, Versa 3D) was used to section the specimen for TEM observation. The site of interest for TEM observation was first coated with a protective carbon film (C-depo) and then milled to produce a thin foil (approximately 70 nm thick) with a depth of nearly 10 μm from the C-depo surface. The thin foil used for TEM observation was secured on a copper grid and then transferred to the chamber of the TEM system equipped with an EDS detector and a high-angle annular dark-field (HAADF) detector.

3. Results

Figs. 1(a-d) show an SEM image and EDS element maps for the Mg-10Al-5Ca alloy. The lamellar structure is a eutectic structure consisting of α-Mg and intermetallic phases with bright contrast. It has been reported that Mg-Al-Ca ternary alloys with similar compositions to the Mg-10Al-5Ca alloy undergo the eutectic transformation L $\rightarrow$ α + C14 + C36 [33]. In this study, we attempted to identify the intermetallic compounds using Kikuchi patterns obtained by EBSD. **Figs. 1(e-h)** show an image quality (IQ) map and inverse pole figure (IPF) maps for the α, C36, and C14 phases, respectively. In addition to the α phase, the C36 and C14 phases were detected, and the predominant intermetallic compound is the C36 phase.

Fig. 2 shows the time evolution of the specimen temperatures of AZ31 (Mg-2.7Al-0.4Zn (at.%)), AZX912 (Mg-8.3Al-0.4Zn-1.2Ca (at.%)), and Mg-10Al-5Ca alloys during ignition temperature measurements with a heating rate of 50 K/min in air. The temperature of each specimen increases approximately linearly with increasing TG-DTA heater temperature until there is a sharp rise, indicating the ignition of the specimen. Mg-10Al-5Ca alloy exhibited the highest ignition temperature of 1436 K, in comparison with 998 K for AZX912 and 882 K for AZ31.

Fig. 3 shows the GI-XRD pattern for the surface of the Mg-10Al-5Ca alloy that was remelted at 973 K for 10 min and then solidified in air. Peaks originating from the α-Mg matrix, C14, C36, CaO, and MgO were clearly detected [34]. On the basis of thermodynamics, the formation of several complex oxides such as $MgAl_2O_4$ and $Ca_3MgAl_4O_{10}$ during the oxidation of Al- and Ca-containing Mg alloys has been predicted [35]. In fact, Czerwinski reported that $MgAl_2O_4$ was formed in an oxide film of AZ91D oxidized at 820 K [36]. Cheng et al. also reported that $MgAl_2O_4$ was formed in an oxide film of Ca-containing AZ91D oxidized at 973 K, although the addition of Y to the Ca-contaning AZ91D suppressed the

formation of $MgAl_2O_4$ [37]. However, in this study, no complex oxides were detected in the GI-XRD measurement. This result suggests that the addition of a large amount of Ca may suppress the formation of $MgAl_2O_4$.

To clarify the morphology of the surface oxide film formed on molten Mg-10Al-5Ca alloy, an FIB-prepared cross-section specimen of the surface oxide film/underlying alloy interface was observed by TEM as shown in **Fig. 4**. The TEM image, EDS element maps, and selected area electron diffraction (SAED) patterns revealed that the film is composed of two layers: a thin outer layer composed of CaO fine grains with an fcc structure having lattice constant a_0 = 0.482 nm (**Fig. 4(c)**) and a thick inner layer composed of MgO with an fcc structure having lattice constant a_0 = 0.421 nm. The thick inner layer was found to have a fine grain region (intermediate layer, **Fig. 4(d)**) and a coarse grain region (innermost layer, **Fig. 4(e)**).

The oxide film layers were also investigated using STEM/EDS. An HAADF image and EDS element maps for Mg, Al, Ca, and O are shown in **Figs. 4(h-l)**, respectively. Ca element was detected in the outer and intermediate layers. A significant amount of Ca is concentrated in the outer layer. Mg element was detected in the intermediate and innermost layers. A very small amount of Al was detected in the intermediate layer, which appeared to exist adjacent to the Ca. However, no complex oxides were detected at this location by SAED measurement. The cationic fractions of the outer, intermediate, and innermost layers are summarized in **Table 1**. The MgO and CaO appeared to be immiscible with each other. This result agrees with the MgO-CaO binary phase diagram reported previously [38].

4. Discussion

From the results of the GI-XRD measurement, TEM observation, and an Ellingham diagram [39], the possible chemical reactions that occurred on the surface of the molten Mg-10Al-5Ca alloy are as follows.

$$2Mg(l) + O_2(g) = 2MgO(s) \quad (1)$$

$$2Ca(l) + O_2(g) = 2CaO(s) \quad (2)$$

$$MgO(s) + Ca(l) = Mg(l) + CaO(s) \quad (3)$$

The standard Gibbs free energies of reactions (1) and (2) are given as follows [40].

$$\Delta G^0_{(1)} = -1217280 + 230.08T \ \text{[J/mol of } O_2\text{]} \quad (4)$$

$$\Delta G^0_{(2)} = -1285360 + 222.20T \ \text{[J/mol of } O_2\text{]} \quad (5)$$

From equations (4) and (5), the standard Gibbs free energy of reaction (3), $\Delta G^0_{(3)}$, can be derived as

$$\Delta G^0_{(3)} = \frac{1}{2}\Delta G^0_{(2)} - \frac{1}{2}\Delta G^0_{(1)} = -34040 - 3.94T \ \text{[J/mol]}. \quad (6)$$

Under practical conditions, the change in the Gibbs free energy of reaction (3) should be calculated by the following equation:

$$\Delta G_{(3)} = \Delta G^{0}_{(3)} + RT \ln \frac{a_{Mg} a_{CaO}}{a_{MgO} a_{Ca}} \quad (7)$$

For simplification, the mole atomic concentrations of Mg and Ca in the molten alloy were substituted for their elemental activities, and the activities of both MgO and CaO were expressed as unity. The preceding calculations reveal the relationship between changes in the Gibbs free energy of reaction (3), $\Delta G_{(3)}$, and the Ca content of the Mg-10Al-Ca alloy as shown in **Fig. 5(a)**. Changes in $\Delta G_{(3)}$ and equilibrium concentration of Ca as functions of temperature are shown in **Fig. 5(b)**. $\Delta G_{(3)}$ (973 K) has a negative value of -14.95 kJ/mol, which indicates that CaO predominates over MgO on the surface of the molten Mg-10Al-5Ca alloy at 973 K. The equilibrium concentration of Ca in the Mg-Al-Ca melt at 973 K was estimated to be approximately 0.83 at.%. The existence of more than 0.83 at.% Ca in the molten Mg alloy appears to prevent the formation of MgO. However, when the Ca concentration decreases to less than the equilibrium level owing to the consumption of Ca by the formation of a CaO layer, the formation of MgO will occur. After covering the surface with an initial oxide film of CaO, the inner oxide film grows through the diffusion of ions. It has been reported that the outward diffusion rate of Mg^{2+} ions is much higher than the inward diffusion rate of O^{2-} ions [41, 42]. The growth of the inner layer beneath the fine CaO outer layer may be controlled by the outward diffusion of Mg^{2+} ions through the oxide film. We have been investigating the phenomenon of oxide film growth on the surface of Mg alloys from a kinetic viewpoint and plan to publish part of the results shortly.

The outstanding incombustibility of the Mg-10Al-5Ca alloy may be due to the formation of the fine CaO outer layer. The volume ratio of metal oxide to metal, the Pilling-Bedworth (PB) ratio, R_{PB}, has often been used to discuss the formability and effectiveness of a protective corrosion layer [43]. The PB ratio is defined as

$$R_{PB} = \frac{V_{ox}}{V_{m}} = \frac{\left(M_{ox}/r_{ox}\right)}{n\left(M_{m}/r_{m}\right)} \quad , \quad (8)$$

where M is the molar mass [g/mol], ρ is the density [g/cm^3], n is the number of metal atoms per molecule of the oxide, and V is the molar volume [cm^3/mol]. The PB ratio is the ratio of the volume occupied by a metal atom in the oxide to the volume occupied by the same metal atom in the substrate. The PB ratios of MgO/Mg and CaO/Ca are known to be 0.80 and 0.64, respectively [44]. However, in this study, the oxide/alloy interface should also be considered. The PB ratios for MgO/Mg-10Al-5Ca and CaO/Mg-10Al-5Ca were estimated to be 0.77 and 1.17, respectively. Furthermore, this study deals with not only an oxide/alloy interface but

also the oxide/oxide interface of CaO/MgO. Since the type of cation is different in the two oxides, the anionic volume (AV) ratio, R_{AV} [45], is adopted to compare the volume occupied by an oxygen atom in CaO with the volume occupied by an oxygen atom in MgO,

$$R_{AV} = \frac{V_{ox1}}{V_{ox2}} = \frac{n_{ox2}\left(M_{ox1}/r_{ox1}\right)}{n_{ox1}\left(M_{ox2}/r_{ox2}\right)} \quad , \tag{9}$$

where n_{ox} is the number of oxygen atoms per molecule of the oxide. The AV ratio for CaO/MgO was estimated to be 1.48. The estimated ratios for CaO/Mg-10Al-5Ca and CaO/MgO of more than 1 indicate the generation of a strong compressive force in the CaO layer, inhibiting the inward diffusion of oxygen in the layer.

5. Conclusions

The incombustibility of cast Mg-10Al-5Ca alloy was evaluated and the structure of the oxide film formed on the molten alloy was observed by TEM. The obtained results are as follows:

(1) The Mg-10Al-5Ca alloy exhibits a high ignition temperature of 1436 K, in comparison with 998 K for AZX912 and 882 K for AZ31.

(2) The oxide film formed on molten Mg-10Al-5Ca alloy was found to have a three-layered structure consisting of a fine CaO outer layer, a fine MgO intermediate layer, and a coarse MgO innermost layer.

(3) The anionic volume ratio of the CaO/MgO interface was estimated to be 1.48. This large value indicates the generation of a strong compressive force in the CaO layer. The dense and uniform fine CaO layer plays an important role in preventing the diffusion of oxygen.

Acknowledgements

This study is supported by grants-in-aid for Scientific Research (A) No. 23246122 and (B) No. 25289251 from the MEXT Japan. One of the authors (M.Y.) is grateful to the JSPS Program for Advancing Strategic International Networks to Accelerate the Circulation of Talented Researchers.

References

[1] T. M. Pollock, Weight Loss with Magnesium Alloys, Science, 328 (2010) 986-987.

[2] T.R. Marker, Evaluating the Flammability of Various Magnesium Alloys, During Laboratory- and Full-scale Aircraft Fire Test, DOT/FAA/AR-11/3, U.S. Dept. of Transportation, Federal Aviation Administration, Atlantic City, N.J. 2013.

[3] F. Czerwinski, Overcoming Barriers of Magnesium Ignition and Flammability, Adv. Mater. Proc., May, 2014, pp. 28-31.

[4] F. Czerwinski, Controlling the ignition and flammability of magnesium for aerospace applications, Corros. Sci. 86 (2014), 1-16.

[5] M. Liu, D.S. Shih, C. Parish, A. Atrens, The ignition temperature of Mg alloys WE43, AZ31 and AZ91, Corros. Sci. 54 (2012) 139-142.

[6] A. Prasad, Z. Shi, A. Atrens, Influence of Al and Y on the ignition and flammability of Mg alloys, Corros. Sci. 55 (2012) 153-163.

[7] F. Czerwinski, Oxidation Characteristics of Magnesium Alloys, JOM, 64 (2012), 1477-1483.

[8] K.B. Wikle, Improving Aluminum Castings with Beryllium, AFS Trans. 78-119 (1978), 513-518.

[9] C. Houska, Beryllium in aluminum and magnesium alloys, Met. Mater. 2 (1988), 100-104.

[10] G. Foerster, A new approach to magnesium die casting, Adv. Mater. Process. 154 (1998), 79-81.

[11] X. Zeng, Q.Wang, Y.Lu, W. Ding, Y. Zhu, C. Zhai, C. Lu, X. Xu, Behavior of surface oxidation on molten Mg–9Al–0.5Zn–0.3Be alloy, Mater. Sci. Eng. A 301 (2001), 154-161.

[12] Q. Tan, N. Mo, B. Jiang, F. Pan, A. Atrens, M.X. Zhang, Oxidation resistance of Mg–9Al–1Zn alloys micro-alloyed with Be, Scr. Mater. 115 (2016), 38-41.

[13] B.H. Choi, I.M. Park, B.S. You, W.W. Park, Effects of Ca and Be Addition on High Temperature Oxidation Behavior of AZ91 alloys, Mater. Sci. Forum, 419-422 (2003), 639-644.

[14] S. Akiyama, Flame-resistant magnesium alloys by calcium, J. Jpn Foundry Eng. Soc. 68 (1994), 38-42 (in Japanese).

[15] M. Sakamoto, S. Akiyama, K. Ogi, Suppression of ignition and burning of molten Mg alloys by Ca bearing stable oxide film, J. Mater. Sci. Lett. 16 (1997), 1048-1050.

[16] B.S. You, W.W. Park, I.S. Chung, The effect of calusium additions on the oxidation behavior in magnesium alloys, Scr. Mater. 42 (2000), 1089-1094.

[17] B.H. Choi, B.S. You, W.W. Park, Y.B. Huang, I.M. Park, Effect of Ca Addition on the Oxidation Resistance of AZ91 Magnesium Alloys at Elevated Temperatures, Met. Mater. Int. 9 (2003), 395-398.

[18] S.L. Cheng, G.C. Yang, J.F. Fan, Y.J. Li, Y.H. Zhou, Effect of Ca and Y additions on oxidation behavior of AZ91 alloy at elevated temperatures, Trans. Nonferrous Met. Soc. China, 19 (2009), 299-304.

[19] D.B. Lee, Effect of CaO and Hot Extrusion on the Oxidation of AZ61 Magnesium Alloys, Oxid Met. 85 (2016), 65-74.

[20] B.S. You, M.H. Kim, W.W. Park, I.S. Chung, Effects of Al and Y Additions on the Oxidation Behavior of Mg-Ca Base Molten Alloys, Mater. Sci. Forum, 419-422 (2003), 581-586.

[21] J.F. Fan, Z. Chen, W.D. Yang, S. Fang, B.S. Xu, Effect of yttrium, calcium and zirconium on ignition-proof principle and mechanical properties of magnesium alloys, J. Rare Earths, 30 (2012) 74-78.

[22] J.F. Fan, G.C. Yang, S.L. Cheng, H. Xie, W.X. Hao, M. Wang, and Y.H. Zhou, Surface Oxidation Behavior of Mg-Y-Ce Alloys at High Temperature, Metall. Mater. Trans. A, 36A (2005), 235-239.

[23] X.M. Wang, X.Q. Zeng, Y. Zhou, G.S. Wu, S.S. Yao, Y.J. Lai, Early oxidation behaviors of Mg–Y alloys at high temperatures, J. Alloys Comp. 460 (2008), 368-374.

[24] J.F. Fan, C.L. Yang, G. Han, S. Fang, W.D. Yang, B.S. Xu, Oxidation behavior of ignition-proof magnesium alloys with rare earth addition, J. Alloys Comp. 509 (2011), 2137-2142.

[25] Q. Wang, W. Chen, X. Zeng, Y. Lu, W. Ding, Y. Zhu, X. Xu, M. Mabuchi, Effects of Ca addition on the microstructure and mechanical properties of AZ91magnesium alloy, J. Mater. Sci. 36 (2001), 3035-3040.

[26] I.A. Anyanwu, Y. Gokan, A. Suzuki, S. Kamado, Y. Kojima, S. Takeda, T. Ishida, Effect of substituting cerium-rich mischmetal with lanthanum on high temperature properties of die-cast Mg-Zn-Al-Ca-RE alloys, Mater. Sci. Eng. A, 380 (2004), 93-99.

[27] K. Hirai, H. Somekawa, Y. Takigawa, K. Higashi, Effects of Ca and Sr addition on mechanical properties of a cast AZ91 magnesium alloy at room and elevated temperature, Mater. Sci. Eng. A, 403 (2005), 276-280.

[28] A. Suzuki, N.D. Saddock, J.R. Terbush, B.R. Powell, J.W. Jones, T.M. Pollock, Precipitation Strengthening of a Mg-Al-Ca–Based AXJ530 Die-cast Alloy, Metall. Mater. Trans. A, 39A (2008) 696-702.

[29] T. Homma, C.L. Mendis, K. Hono, S. Kamado, Effect of Zr addition on the

mechanical properties of as-extruded Mg-Zn-Ca-Zr alloys, Mater. Sci. Eng. A, 527 (2010), 2356-2362.

[30] S.W. Xu, K. Oh-ishi, H. Sunohara, S. Kamado, Extruded Mg–Zn–Ca–Mn alloys with low yield anisotropy, Mater. Sci. Eng. A, 558 (2012) 356-365.

[31] Y. Kawamura, K. Hayashi, J. Koike, A. Inoue, T. Masumoto, High Strength Nanocrystalline Mg-Al-Ca Alloys Produced by Rapidly Solidified Powder Metallurgy Processing, Mater. Sci. Forum, 350 (2000), 111-116.

[32] Y. Kawamura, Flame-resistant Magnesium Alloys with High Strength, In: Proceedings of the seventh triennial international fire & cabin safety research conference, Philadelphia Marriott Downtown, December 2-5, 2013. https://www.fire.tc.faa.gov/2013Conference/proceedings.asp

[33] A. Suzuki, N.D. Saddock, J.W. Jones, T.M. Pollock, Solidification paths and eutectic intermetallic phases in Mg-Al-Ca ternary alloys, Acta Mater. 53 (2005) 2823-2834.

[34] T. Rzychon, Characterization of Mg-rich clusters in the C36 phase of the Mg-5Al-3Ca-0.7Sr-0.2Mn alloy, J. Alloy. Compd. 598 (2014), 95-105.

[35] S. I. Shornikov, Thermodynamic property of CaO-MgO-Al_2O_3 melts, Vestn. Otd. nauk Zemle, 3, NZ6100, doi:10.2205/2011NZ000230 (2011)

[36] F. Czerwinski, The oxidation behavior of an AZ91D magnesium alloy at high temperatures, Acta Mater. 50 (2002), 2639-2654.

[37] S.L Cheng, G.C. Yang, J.F. Fan, Y.J. Li, Y.H. Zhou, effect of Ca and Y additions on oxidation behavior of AZ91D alloy at elevated temperatures, Trans. Nonferrous Met. Soc. China, 19 (2009), 299-304.

[38] R.C. Doman, J. B. Barr, R. N. McNally, A. M. Alper, Phase Equilibria in the System CaO-MgO, J. Am. Ceram. Soc., 46 (1963), 313-316.

[39] H. J. T. Ellingham, Reducibility of oxides and sulphides in metallurgical processes, Trans. Comm., J. Soc. Chem. 63 (1944), 125-160.

[40] O. Knacke, O. Kubaschewski, K. Hesselmann, Thermochemical Properties of Inorganic Substances, 2nd ed., Springer-Verlag, Verlag Stahleisen, 1991.

[41] M.H. Zayan, Model for Nonprotective Oxidation of AI-Mg Alloys, Oxid. Met. 34 (1990) 465-472.

[42] O. Salas, H. Ni, V. Jayaram, K.C. Vlach, C.G. Levi, R. Mehrabian, Nucleation and growth of Al_2O_3/metal composites by oxidation of aluminum alloys, J. Mater. Res. 6 (1991) 1964-1981.

[43] N.B. Pilling, R.E. Bedworth, The Oxidation of Metals at High Temperatures, J.Inst. Met. 29 (1923) 529-582.

[44] C.A.C. Sequeira, High-Temperature Oxidation, in: R. Winston Revie (Ed.), Uhlig's Corrosion Handbook, Third Edition, John Wiley & Sons, Inc., New Jersey, 2011, pp. 247-280.

[45] T.E. Mitchell, D.A. Voss, E.P. Butler, The observation of stress effects during the high temperature oxidation of iron, J. Mater. Sci. 17 (1982) 1825-1833.

Figure Captions

Fig. 1 (a) SEM image of a cast Mg-10Al-5Ca alloy and its EDS element maps for (b) Mg, (c) Al, and (d) Ca. (e) EBSD IQ map and IPF maps for (f) α, (g) C36, and (h) C14 phases.

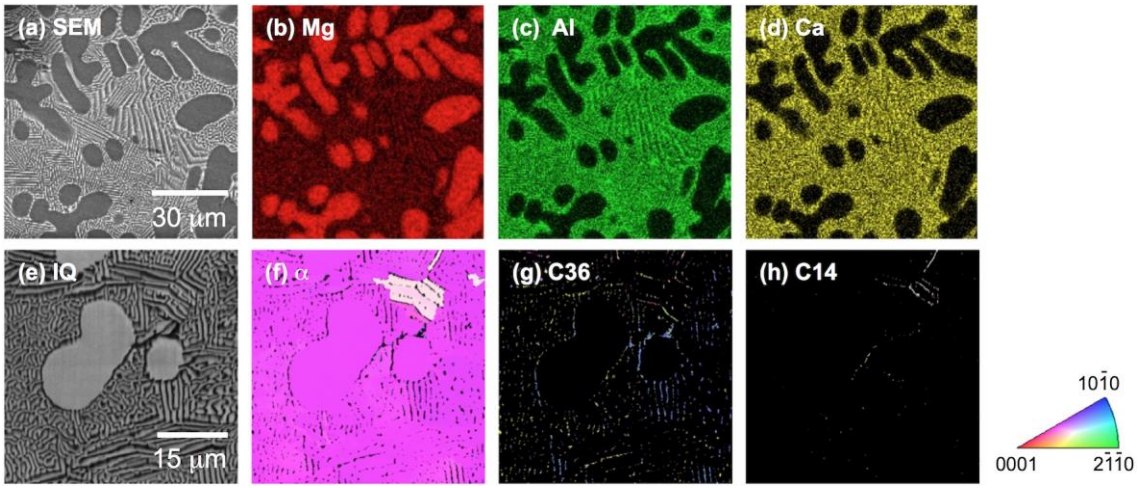

Fig. 2 Time evolution of specimen temperatures of AZ31, AZX912, and Mg-10Al-5Ca (at.%) during ignition temperature measurements with a heating rate of 50 K/min in air.

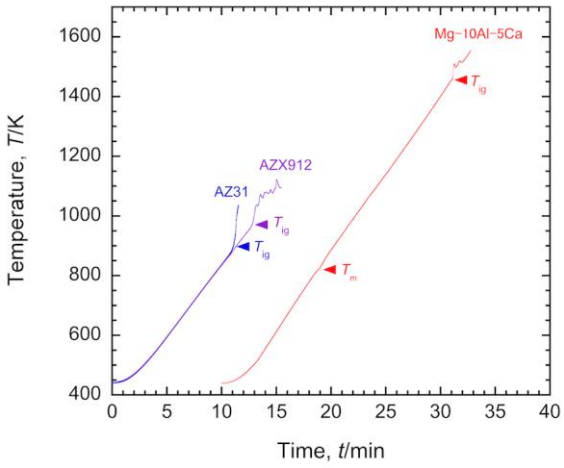

Fig. 3 Grazing incidence XRD pattern for the surface of Mg-10Al-5Ca alloy remelted at 973 K for 10 min and then solidified in air. The incident angle was 0.2°.

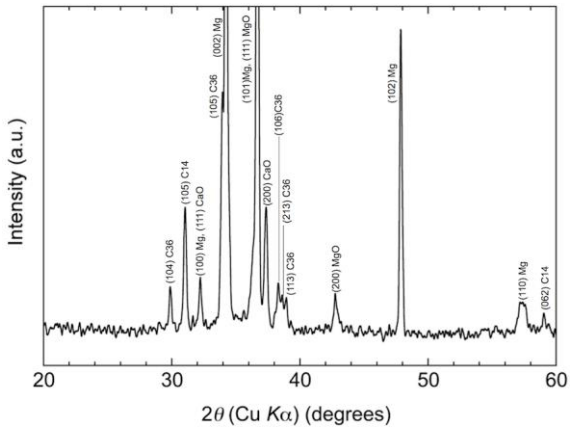

Fig. 4 (a) TEM image of an FIB-prepared cross section of the film formed on the alloy after solidification of the molten Mg-10Al-5Ca alloy. (b) Schematic diagram of layered structure of the oxide film. SAED patterns obtained from each region; (c) outer layer, (d) intermediate layer, (e) innermost layer, (f) underlying alloy, and (g) intermetallic compound. (h) HAADF image and EDS element maps for (i) Mg, (j) Al, (k) Ca, and (l) O elements.

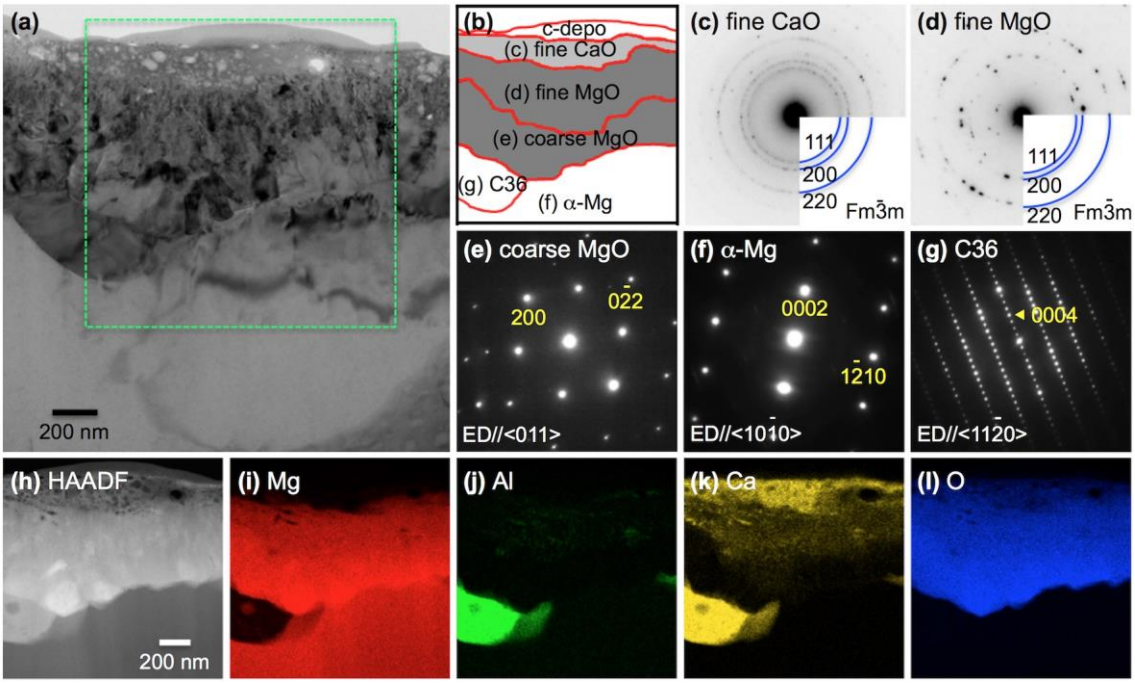

Fig. 5 (a) Relationship between ΔG of the reaction MgO(s) + Ca(l) = Mg(l) + CaO(s) at 973 K and Ca content of Mg-10Al-Ca and Mg-Ca alloys. (b) Changes in ΔG and equilibrium concentration of Ca as functions of temperature.

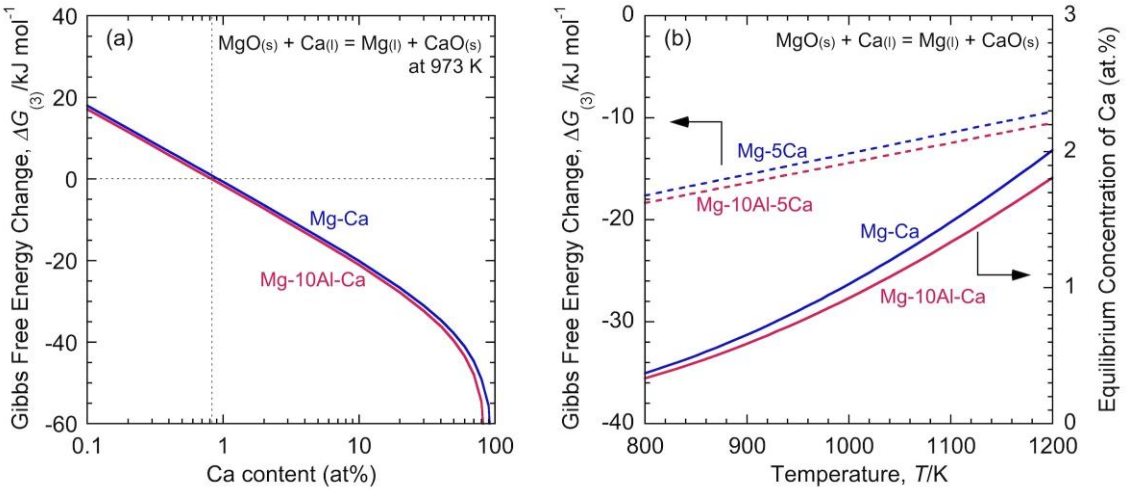

Table 1 Cationic fractions of outer, intermediate, and innermost layers in the oxide film formed on molten Mg-10Al-5Ca alloy.

Table 1 Cationic fractions of outer, intermediate, and innermost layers in the oxide film formed on a molten Mg-10Al-5Ca alloy.

layer	Cationic fraction		
	Mg	Al	Ca
Outer	0.083±0.048	0.012±0.002	0.905±0.049
Intermediate	0.926±0.009	0.02±0.006	0.053±0.007
Innermost	0.995±0.001	<0.003	<0.002